

## Onset of long-range order in superlattices: Mean-field theory

R. W. Wang and D. L. Mills

*Department of Physics, University of California, Irvine, Irvine, California 92717*

(Received 18 February 1992)

We discuss the onset of long-range order in a model superlattice that consists of two materials, each of which undergoes a phase transition, in bulk form. We suppose that each transition has Ising character, and describe the onset of long-range order, along with the response to a uniform external field, by use of Landau-Ginzburg theory. The issue explored is the circumstances under which the structure displays a single maximum (singularity) in the susceptibility, and those in which two maxima (one maximum, one singularity) appear, near the bulk transition temperature of each constituent. The analysis is motivated by experimental studies of a  $\text{CoF}_2/\text{FeF}_2$  superlattice reported by Jaccarino and co-workers.

### I. INTRODUCTION

Currently it is possible to synthesize superlattices from a diverse array of materials, ranging from semiconductors to metals within which superconductivity or magnetic order may appear. In this way, one may fabricate new artificial materials with properties not shared by any single constituent.

Quite clearly, the superlattice will behave as a coherent structure, or a new material, if the films are sufficiently thin. But if one envisions increasing the thickness of each of the two films within a superlattice unit cell, eventually each material will acquire response characteristics of its bulk form, and the superlattice will behave as a collection of films of two bulk materials, rather than a single new artificial material. The description of the transition between these two regimes is, in our view, an interesting theoretical issue.

This question is addressed in the experimental studies of  $\text{FeF}_2/\text{CoF}_2$  superlattices reported by Ramos, Lederman, King, and Jaccarino.<sup>1</sup> Each material, in its bulk form, is a uniaxial antiferromagnet. The bulk transition temperature of  $\text{FeF}_2$  is 78 K, and that of  $\text{CoF}_2$  is about 39 K. In one superlattice consisting of 19 atomic layers of  $\text{FeF}_2$  and 6 of  $\text{CoF}_2$ , these authors report a single magnetic phase transition at a temperature slightly below that of  $\text{FeF}_2$  in the bulk. There is no evidence of any structure in the thermodynamic properties studied (the thermal expansion) in the vicinity of the bulk  $\text{CoF}_2$  transition temperature. One may say that this sample is a new magnetic material with a single coherent phase transition in which long-range order extends throughout the structure below a single transition temperature. Conversely, a sample with 25 layers of  $\text{FeF}_2$  and 30 layers of  $\text{CoF}_2$  displays two anomalies in the thermal expansion, one near (but below) the bulk  $\text{FeF}_2$  transition temperature, and one near (but above) that of  $\text{CoF}_2$ . Loosely speaking, the data suggest that the second sample behaves magnetically as a collection of  $\text{FeF}_2$  films and  $\text{CoF}_2$  films that are only weakly coupled, and which display magnetic phase transitions rather similar to each bulk material.

This paper is devoted to the study of a model superlattice of films  $A$  and  $B$ ; within the bulk form of  $A$  we have

a phase transition at temperature  $T_A^{(\infty)}$ , and within the bulk form of  $B$  we have a phase transition at  $T_B^{(\infty)}$ , where  $T_A^{(\infty)} > T_B^{(\infty)}$ . We outline, within Landau-Ginzburg theory, the behavior of the superlattice in the two regimes illustrated in the experiments described above, and we provide a description of the transition between the two regimes. We calculate the temperature variation of the order parameter for our model along with its linear response to a spatially uniform external field. We regard the issues examined here as of general interest; this is the motivation for our use of Landau-Ginzburg theory rather than an explicit microscopic model of the particular materials studied in Ref. 1. The issue explored here will arise, for example, in layered superconductors. We note the Carriço and Camley<sup>2</sup> have recently developed a microscopic model of  $\text{FeF}_2/\text{CoF}_2$  superlattices and explored its behavior in zero external magnetic field.

We note that as the temperature is lowered, the structure can exhibit only one true thermodynamic phase transition, and below this temperature long-range order exists everywhere in the superlattice. Suppose we are in the regime where there are two distinct maxima in the linear susceptibility  $\chi$ , one at  $T_A$  near  $T_A^{(\infty)}$ , and one at  $T_B$ , near  $T_B^{(\infty)}$ ; recall  $T_A^{(\infty)} > T_B^{(\infty)}$ , so we will have  $T_A > T_B$ . Above  $T_A$  there is no order anywhere, and below  $T_A$  order sets in; the linear susceptibility  $\chi$  displays a true singularity. Now just below  $T_A$ , if the  $B$  films are thick, the order parameter in the  $B$  films will be appreciable only near the interfaces. Its magnitude will decay exponentially as one moves away from the interface into any given  $B$  film. But the order parameter  $\eta_B$  in the  $B$  film is nonzero everywhere throughout the film, even if it may be very small near the center. Then the second feature in  $\chi$  at the lower temperature  $T_B$  cannot be a singularity, rather, it will be a feature with a finite maximum. There is a narrow region of temperature near  $T_B$  where the structure exhibits a strongly enhanced response to an external field, and there will be "near singularities" in its thermodynamic properties. In this narrow temperature region, the order parameter in film  $B$  grows rapidly. We shall study here the development of this feature with increasing film thickness. In Sec. II, we discuss the Landau-Ginzburg equations that form the

basis of this calculation, and the results are presented in Sec. III.

## II. THEORETICAL ANALYSIS

### A. General Considerations

The model we are considering is illustrated in Fig. 1. We have a superlattice that consists of two materials  $A$  and  $B$ ; the thickness (in atomic layers) of the films of material  $A$  is  $N_A$ , and that of the films of material  $B$  is  $N_B$ . The number of films in each unit cell is then  $N_A + N_B$ . Material  $A$ , in bulk form, undergoes a phase transition at temperature  $T_A^{(\infty)}$ , and material  $B$  at temperature  $T_B^{(\infty)}$ . Throughout this discussion, we assume  $T_A^{(\infty)} > T_B^{(\infty)}$ , as mentioned above. Each phase transition is described by scalar order parameters  $\eta_A$  and  $\eta_B$ , respectively. If we wish to consider two ferromagnets, then  $\eta_A$  and  $\eta_B$  are the magnetizations of the respective materials. An example of a particular system of this nature to which the present theory would apply would be Fe/Ni superlattice. Heinrich *et al.* have fabricated Fe/Ni bilayers on Ag(001),<sup>3</sup> and it should prove possible to synthesize a complete superlattice. The bilayers have been studied only well below their transition temperature. Whether or not these materials could be studied at high temperatures, near the Curie point, would depend on the structure's ability to maintain its integrity well above room temperature. If the theory is applied to the superlattices studied, fabricated from the uniaxial antiferromagnets CoF<sub>2</sub> and FeF<sub>2</sub>, then  $\eta_A$  and  $\eta_B$  are the staggered magnetizations of each material. Finally, we can discuss superconducting structures, within which  $\eta_A$  and  $\eta_B$  are the pair amplitudes.<sup>4</sup> The present theory ignores phase fluctuations, and thus in this case can apply to sufficiently thick superconducting films.

Each material is described by a free-energy density we write in the form, with  $H_{\text{ex}}$  a spatially uniform external field that couples to the order parameter,<sup>4</sup>

$$F_i = \frac{1}{4}c_i \left[ \frac{\partial \eta_i}{\partial x} \right]^2 + \frac{1}{2}a_i(T)\eta_i^2 + \frac{1}{4}b_i(T)\eta_i^4 - H_{\text{ex}}\eta_i, \quad (1)$$

where  $i$  stands for  $A$  or  $B$ , and the measure of length  $x$  is dimensionless, with the spacing between adjacent planes chosen to be unity. In the spirit of Landau-Ginzburg theory,  $b_i$  and  $c_i$  are independent of temperature, while  $a_i = a'_i(T - T_i^{(\infty)})$ . The spatial variation of the order parameter in each medium is then controlled by

$$-\frac{1}{2}c_i \frac{\partial^2 \eta_i}{\partial x^2} + a'_i(T - T_i^{(\infty)})\eta_i + b_i\eta_i^3 = H_{\text{ex}}. \quad (2)$$

We rescale various quantities in Eq. (2). Below the bulk ordering temperature, in the infinite medium, the order parameter is  $\eta_i^{(\infty)} = (a'_i/b_i)^{1/2}(T_i^{(\infty)} - T)^{1/2}$ . We let  $\eta_i = f_i(x)\eta_i^{(\infty)}$ , where above  $T_i^{(\infty)}$  we write  $\eta_i^{(\infty)} = (a'_i/b_i)^{1/2}(T - T_i^{(\infty)})^{1/2}$ . We then encounter the temperature-dependent coherence length  $\xi_i(T) = \xi_i^{(0)}(T_i^{(\infty)} - |T_i^{(\infty)} - T|)^{1/2}$ , where  $\xi_i^{(0)} = (c_i/a'_i T_i^{(\infty)})^{1/2}$ .

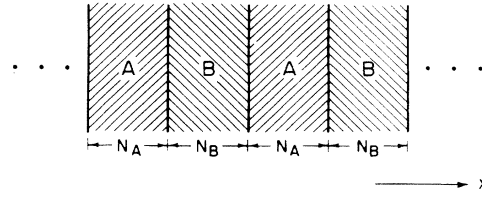


FIG. 1. Model superlattice structure described in the text.

We may rewrite Eq. (2) in the form

$$-\frac{\xi_i^2}{2} \frac{d^2 f_i}{dx^2} - \nu_i f_i + f_i^3 = h_{\text{ex}}, \quad (3)$$

where  $\nu_i = \text{sgn}(T_i^{(\infty)}/T - 1)$ . Here  $h_{\text{ex}} = H_{\text{ex}}/b_i(\eta_i^{(\infty)})^3$ .

One may resort to specific models of particular systems to generate estimates for the parameters that enter the Landau-Ginzburg functional in Eq. (1). With ferromagnetic superlattices in mind, consider BCC Heisenberg films, with nearest-neighbor exchange couplings and interfaces in the superlattice parallel to (100) planes. Expanding the appropriate Brillouin functions in the spirit of mean-field theory gives  $\xi_i^{(0)} = 1$ , and

$$(\eta_i^{(\infty)})^2 = \frac{5}{3} \frac{(S+1)^2}{S(S+1) + \frac{1}{2}} \left| 1 - \frac{T}{T_i^{(\infty)}} \right|. \quad (4)$$

Quite generally, in magnetic materials the low-temperature coherence length  $\xi_i^{(0)}$  is indeed the order of a lattice constant, while in superconductors it may range from a few lattice constants to  $10^4$  in clean conventional superconductors.

So the spatial variations of the order parameter within each film are described by Eq. (3). We then require a boundary condition at each interface. The most general boundary condition will be a linear combination of the derivatives  $(\partial \eta_i / \partial x)$ , and the order parameters  $\eta_i$  themselves.<sup>5</sup> To obtain explicit forms, we resort to the microscopic model mentioned in the previous paragraph; the general structure of our conclusions are not affected by the details of the boundary condition. Consider an interface at  $x = 0$ , with a  $B$  film to the right, and an  $A$  film to the left. If  $J_I$  is the strength of the exchange coupling across the interface, with  $J_A$  and  $J_B$  that in each material, we find

$$\frac{J_I}{J_A} \frac{\xi_A}{\xi_B} f_B(0^+) = f_A(0^-) + \left[ \frac{df_A}{dx} \right]_{0^-} \quad (5a)$$

and

$$\frac{J_I}{J_B} \frac{\xi_B}{\xi_A} f_A(0^-) = f_B(0^+) - \left[ \frac{df_B}{dx} \right]_{0^+}. \quad (5b)$$

Our task is to solve the above set of equations, subject to the constraint that the order parameter displays the periodicity of the superlattice. This is insured if both  $f_A$  and  $f_B$  have zero slopes at the midpoints of their respective films. We then proceed by guessing the value for  $f_A$  at the midpoint of an  $A$  film, integrating the equations forward until we reach the midpoint of the neighboring  $B$

film, then inquiring if the order parameter has a zero slope there. By scanning a range of guesses for  $f_A$ , one may locate a solution. We turn next to a discussion of our numerical procedures, since the calculations are challenging to carry through.

### B. Numerical methods

The results presented below were calculated in two distinct steps. We begin by setting  $H_{\text{ex}}=0$ , and then we find the order parameters  $\eta_i(x)$  by solving the Landau-Ginsburg equations given above. Our means of doing this is discussed below. Then we calculate the linear response of the superlattice to  $H_{\text{ex}}$ . This may be described by introducing the position-dependent susceptibility

$$\chi_i(x) = \frac{\partial \eta_i(x)}{\partial H_{\text{ex}}} . \quad (6)$$

Notice one has also

$$\chi_i(x) = \frac{1}{3} \frac{(S+1)}{k_B} \frac{1}{|T_i^{(\infty)} - T|} \chi_i^{(r)}(x) , \quad (7a)$$

where the reduced susceptibility

$$\chi_i^{(r)}(x) = \left[ \frac{\partial f_i}{\partial h_{\text{ex}}} \right]_0 \quad (7b)$$

obeys the linear differential equation

$$\frac{\xi_i^2}{2} \frac{d^2 \chi_i^{(r)}}{dx^2} + [v_i - 3f_i^2(x)] \chi_i^{(r)} + 1 = 0 , \quad (8)$$

and  $f_i(x)$  is now the order parameter when  $H_{\text{ex}}=0$ . The boundary conditions obeyed by the reduced susceptibility are deduced easily from those obeyed by the order parameter by differentiating Eqs. (5). One can write these in the form

$$\frac{J_I}{J_B} \frac{\xi_B^2}{\xi_A^2} \chi_B^{(r)}(0^+) = \chi_A^{(r)}(0^-) + \left[ \frac{d\chi_A^{(r)}}{dx} \right]_{0^-} \quad (9a)$$

and

$$\frac{J_I}{J_A} \frac{\xi_A^2}{\xi_B^2} \chi_A^{(r)}(0^-) = \chi_B^{(r)}(0^+) - \left[ \frac{d\chi_B^{(r)}}{dx} \right]_{0^+} . \quad (9b)$$

Given the order parameters in zero field  $f_i(x)$ , we may solve Eq. (8), a linear inhomogeneous differential equation, by means of a Green's-function method. Consider  $\chi_A^{(r)}(x)$ , the reduced susceptibility in film  $A$ , which extends from  $x=-N_A$  to  $x=0$ . We introduce  $\chi_A^{(1)}(x)$ ,  $\chi_A^{(2)}(x)$ , which are linearly independent solutions to the

homogeneous version of Eq. (8), and which obey the boundary conditions

$$\left[ \frac{d\chi_A^{(1)}}{dx} \right]_{x=-1/2N_A} = 0, \quad \chi_A^{(1)}(-\frac{1}{2}N_A) = \text{const} , \quad (10a)$$

and

$$\chi_A^{(2)}(0^-) = 0, \quad \left[ \frac{d\chi_A^{(2)}}{dx} \right]_{0^-} = \text{const} , \quad (10b)$$

where the two constants are chosen arbitrarily. The Wronskian  $W_A \equiv \chi_A^{(1)}(x)(d\chi_A^{(2)}/dx) - (d\chi_A^{(1)}/dx)\chi_A^{(2)}(x) = \chi_A^{(1)}(0^-)(d\chi_A^{(2)}/dx|_{0^-})$ . One may then show the reduced susceptibility  $\chi_A^{(r)}(x)$  within film  $A$  is given by

$$\begin{aligned} \chi_A^{(r)}(x) = & \frac{1}{W_A} \chi_A^{(r)}(0^-) \left[ \frac{d\chi_A^{(2)}}{dx} \right]_{0^-} \chi_A^{(1)}(x) \\ & - \frac{2}{\xi_A^2 W_A} \left[ \chi_A^{(1)}(x) \int_x^0 dx' \chi_A^{(2)}(x') \right. \\ & \left. + \chi_A^{(2)}(x) \int_{-1/2N_A}^x dx' \chi_A^{(1)}(x') \right] . \quad (11) \end{aligned}$$

The constant  $\chi_A^{(r)}(0^-)$  is found by submitting Eq. (11) to the boundary conditions once a similar formula for  $\chi_B^{(r)}(x)$  is generated. This may be done, noting film  $B$  extends from  $x=0$  to  $x=N_B$ , by introducing two linearly independent solutions to the homogeneous version of Eq. (8) in film  $B$ . These functions satisfy

$$\left[ \frac{d\chi_B^{(1)}}{dx} \right]_{x=(1/2)N_B} = 0, \quad \chi_B^{(1)}(\frac{1}{2}N_B) = \text{const} , \quad (12a)$$

and

$$\chi_B^{(2)}(0^+) = 0, \quad \left[ \frac{d\chi_B^{(2)}}{dx} \right]_{0^+} = \text{const} . \quad (12b)$$

We then have

$$\begin{aligned} \chi_B^{(r)}(x) = & \frac{1}{W_B} \chi_B^{(r)}(0^+) \left[ \frac{d\chi_B^{(2)}}{dx} \right]_{0^+} \chi_B^{(1)}(x) \\ & + \frac{2}{\xi_B^2 W_B} \left[ \chi_B^{(1)}(x) \int_0^x dx' \chi_B^{(2)}(x') \right. \\ & \left. + \chi_B^{(2)}(x) \int_x^{1/2N_B} dx' \chi_B^{(1)}(x') \right] . \quad (13) \end{aligned}$$

The Wronskian  $W_B = \chi_B^{(1)}(0^+)(d\chi_B^{(2)}/dx|_{0^+})$ . Upon submitting these solutions to the boundary conditions, we find that  $\chi_A^{(r)}(0^-)$  and  $\chi_B^{(r)}(0^+)$  are found by solving two linear algebraic equations. If  $\underline{M}$  is the  $2 \times 2$  matrix

$$\underline{M} = \begin{pmatrix} \xi_A^2 \left[ 1 + \frac{(d\chi_A^{(1)}/dx|_{0^-})}{\chi_A^{(1)}(0^-)} \right] & -\frac{J_I}{J_B} \xi_B^2 \\ -\frac{J_I}{J_A} \xi_A^2 & \xi_B^2 \left[ 1 - \frac{(d\chi_B^{(1)}/dx|_{0^+})}{\chi_B^{(1)}(0^+)} \right] \end{pmatrix} , \quad (14)$$

then

$$\underline{M} \begin{bmatrix} \chi_A^{(r)}(0^-) \\ \chi_B^{(r)}(0^+) \end{bmatrix} = \begin{bmatrix} \frac{2}{\chi_A^{(1)}(0^-)} \int_{-1/2N_A}^0 dx' \chi_A^{(1)}(x') \\ \frac{2}{\chi_B^{(1)}(0^+)} \int_0^{1/2N_B} dx' \chi_B^{(1)}(x') \end{bmatrix}. \quad (15)$$

Once the order parameters in zero field are found, the above scheme proves an efficient and accurate means of generating the response of the superlattice to the external field. Our next task is to discuss the means of obtaining the order parameter in zero field.

We have, as noted earlier,  $T_A^{(\infty)} > T_B^{(\infty)}$ . Thus so long as the exchange coupling between spins across the interface is equal to or less than that in film  $A$  itself, a circumstance we assume in the results presented below, we expect the transition temperature  $T_A$ , at which long-range order sets in, to be less than  $T_A^{(\infty)}$ . We may find an implicit equation for  $T_A$  by examining the linearized Landau-Ginzburg equations, and inquiring when the homogeneous version of these admit a nonzero solution. If  $k_A = \sqrt{2}/\xi_A$ , and  $k_B = \sqrt{2}/\xi_B$ , then the transition temperature is found by locating the zero of the following expression:

$$[\cos(\frac{1}{2}k_A N_A) - k_A \sin(\frac{1}{2}k_A N_A)][\cosh(\frac{1}{2}k_B N_B) + k_B \sinh(\frac{1}{2}k_B N_B)] = \frac{J_I^2}{J_A J_B} \cos(\frac{1}{2}k_A N_A) \cosh(\frac{1}{2}k_B N_B). \quad (16)$$

Above  $T_A$ , the only solution of the Landau-Ginzburg equations with  $H_{ex} = 0$  is  $f_A(x) = f_B(x) = 0$ . For all temperatures below  $T_A$ , one may show that  $0 < f_A(-\frac{1}{2}N_A) < 1$ . Hence as we integrate the Landau-Ginzburg equations numerically, we scan the range  $(0,1)$  in  $f_A(-\frac{1}{2}N_A)$ , searching for solutions where  $(df_A/dx)|_{-1/2N_A} = (df_B/dx)|_{+1/2N_B} = 0$ . While  $f_A(-\frac{1}{2}N_A)$  can never equal to unity precisely, as the temperature is reduced below  $T_A$ , it can be driven very close to unity in value. Under these conditions, and when film  $A$  is rather thick, then  $f_A(x)$  is very close to unity, and varies extremely slowly with  $x$  throughout much of film  $A$ ; direct numerical integration of the Landau-Ginzburg equations becomes very difficult.

Suppose we measure distance from the center of film  $A$  by letting  $\bar{x} = x + \frac{1}{2}N_A$ . Then when  $f_A(\bar{x})$  is close to unity, we write  $f_A(\bar{x}) = 1 - g_A(\bar{x})$ , and treat  $g_A(\bar{x})$  as small. One may expand that solution of the Landau-Ginzburg equation with zero slope at  $\bar{x} = 0$  in powers of  $g_A(0)$ . We find

$$g_A(\bar{x}) = g_A(0) \cosh \left[ \frac{2}{\xi_A} \bar{x} \right] + \frac{g_A^2(0)}{2} \left[ 1 - \cosh \left[ \frac{2}{\xi_A} \bar{x} \right] \right] \times \left[ 2 + \cosh \left[ \frac{2}{\xi_A} \bar{x} \right] \right] + \dots \quad (17)$$

We may select a value for  $g_A(0)$ , then use Eq. (17) to calculate analytically  $f_A(\bar{x})$ ,  $(df_A/dx)_{\bar{x}}$  at some point removed far enough from the film center for the numerical integration to proceed accurately from this point on. In practice, this point may be several coherence lengths from the film center.

In the next section, we will display results for the temperature variation of the order parameter in the struc-

ture, along with the average susceptibility  $\bar{\chi}$  of the structure, which is written in terms of the reduced susceptibilities defined in Eqs. (7):

$$\bar{\chi} = \frac{1}{3} \frac{(S+1)}{k_B} \left\{ \frac{1}{|T_A^{(\infty)} - T|} \int_{-N_A/2}^0 dx \chi_A^{(r)}(x) + \frac{1}{|T_B^{(\infty)} - T|} \int_0^{N_B/2} dx \chi_B^{(r)}(x) \right\}. \quad (18)$$

### III. RESULTS AND DISCUSSION

We now present the results of our calculations, which explore the temperature and spatial variation of the order parameter in the structure, along with the susceptibility defined in Eq. (18). We express results in terms of a reduced temperature, defined as  $\tau = T/T_A^{(\infty)}$ . We have chosen  $T_B^{(\infty)}/T_A^{(\infty)} = 0.5$ , roughly correct for the actual materials studied experimentally, and the interfacial coupling constant  $J_I$  has the value  $J_I = (J_A J_B)^{1/2}$ .

In Fig. 2 we show various quantities calculated for the case where  $N_A = N_B = 1$ , which is a superlattice consisting of alternating single layers of  $A$  spins and  $B$  spins. Clearly, we expect this to be a "new material," with a phase transition at a temperature intermediate between that of  $A$  and  $B$ . The solid line is the susceptibility  $\bar{\chi}$  defined in Eq. (18). We indeed see a singularity centered about the transition temperature determined from Eq. (16). The two dashed lines are the integrated order parameters in the two films,

$$\eta_A^{(\text{TOT})} = \int_{-1/2N_A}^0 dx \eta_A(x), \quad (19a)$$

$$\eta_B^{(\text{TOT})} = \int_0^{1/2N_B} dx \eta_B(x), \quad (19b)$$

and the dotted line is the sum

$$\eta^{(\text{TOT})} = \eta_A^{(\text{TOT})} + \eta_B^{(\text{TOT})}. \quad (20)$$

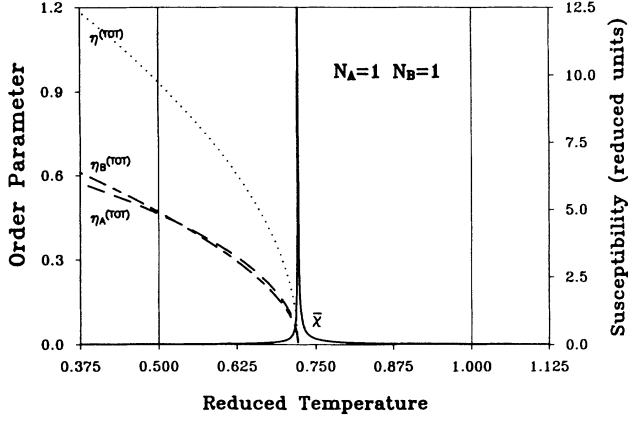


FIG. 2. Temperature variation of the susceptibility and order parameters for a model superlattice with  $N_A = N_B = 1$ . The solid line is the susceptibility, the long-dashed line is  $\eta_A^{(TOT)}$  as defined in Eq. (19a), the short-dashed-long-dashed line is  $\eta_B^{(TOT)}$ , as defined in Eq. (19b), and the dotted line is  $\eta^{(TOT)}$ , Eq. (20). In reduced units,  $T_A^{(\infty)} = 1$ ,  $T_B^{(\infty)} = 0.50$ , and  $T_A = 0.7215$ .

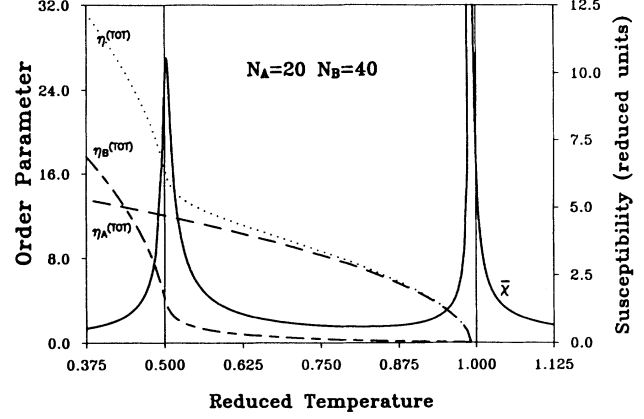


FIG. 5. Same as Fig. 2, except now  $N_A = 20$ ,  $N_B = 40$ , and  $T_A = 0.9910$ ,  $T_B = 0.5021$ .

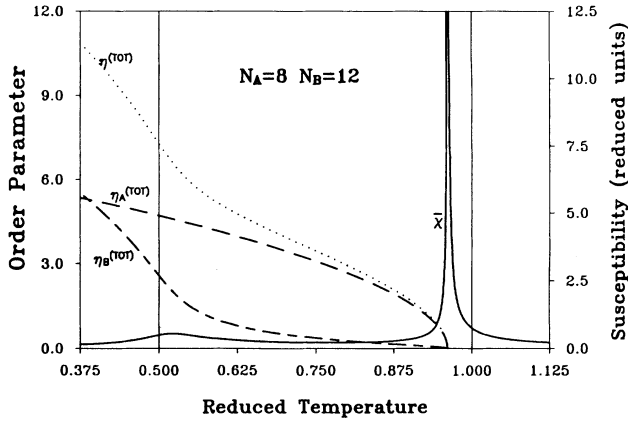


FIG. 3. Same as Fig. 2, except now  $N_A = 8$ ,  $N_B = 12$ , and  $T_A = 0.9609$ ,  $T_B = 0.5216$ .

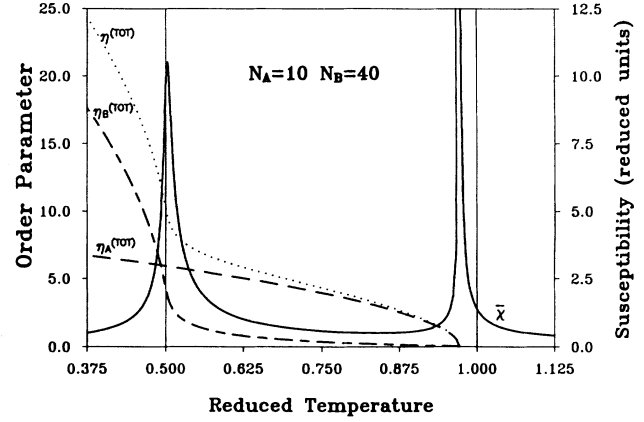


FIG. 6. Same as Fig. 2, except now  $N_A = 10$ ,  $N_B = 40$ , and  $T_A = 0.9720$ ,  $T_B = 0.5020$ .

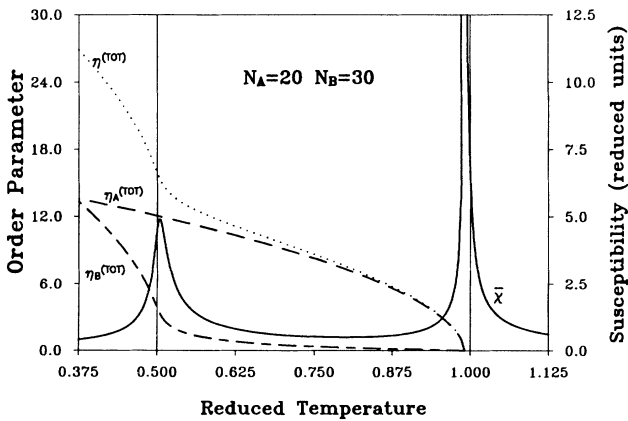


FIG. 4. Same as Fig. 2, except now  $N_A = 20$ ,  $N_B = 30$ , and  $T_A = 0.9910$ ,  $T_B = 0.5034$ .

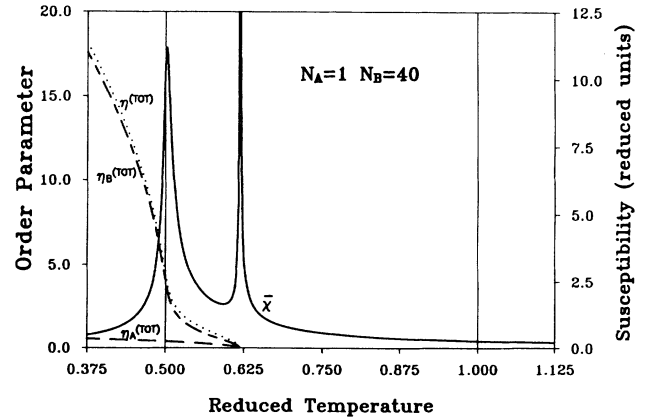


FIG. 7. Same as Fig. 2, except now  $N_A = 1$ ,  $N_B = 40$ , and  $T_A = 0.6185$ ,  $T_B = 0.5025$ .

If these were two ferromagnetic films, ferromagnetically coupled, then  $\eta^{(\text{TOT})}$  would be the total magnetization of (half) the superlattice unit cell.

As we increase the film thicknesses, the singularity in  $\bar{\chi}$  moves up toward  $T_A^{(\infty)}$ , as we see in Fig. 3, calculated for  $N_A=8$  and  $N_B=12$ . We can begin to see the development of a very modest structure in  $\bar{\chi}$  just above  $T_B^{(\infty)}$  for this case. There is a broad but distinct maximum in  $\bar{\chi}$ , and in this region  $\eta_B^{(\text{TOT})}$  has a slope that increases rapidly in magnitude. We are surprised by the very modest structure in  $\bar{\chi}$  near  $T_B^{(\infty)}$ , even though  $N_B$  is now quite large compared to unity (recall that the coherence length in material  $B$  far from  $T_B^{(\infty)}$  is quite close to one inter-layer spacing). This result is compatible with the data reported in Ref. 1. The data suggest the  $\text{CoF}_2$  film must have a thickness in the range of 30 layers for a low-temperature "transition" to be evident.

Figure 4 displays calculations for  $N_A=20$  and  $N_B=30$ . We see a clear, well-defined maximum in  $\bar{\chi}$ ; there is no singularity in this quantity, and as a consequence one does not realize two "phase transitions" in the structure, but the desire of the  $B$  films to order spontaneously near  $T_B^{(\infty)}$  is evident. Also, as the temperature is lowered below the maximum,  $\eta_B^{(\text{TOT})}$  begins to increase rapidly with temperature, a behavior seen clearly in  $\eta^{(\text{TOT})}$ . We continue on to the case where  $N_B=40$  in Fig. 5, where we see a very prominent feature in  $\bar{\chi}$ . Also,  $\eta^{(\text{TOT})}$  shows a clear feature near the maximum in  $\bar{\chi}$ .

If we hold the number of  $B$  layers fixed, but decrease  $N_A$ , the onset of long-range order in the system occurs at a progressively lower temperature. We show this in Fig. 6 and Fig. 7 for the cases  $N_A=10$  and  $N_B=40$ , and  $N_A=1$  and  $N_B=40$ . For the latter case, we still see two clear features in  $\bar{\chi}$ . Here we have spontaneous order in the  $A$  monolayers, treated here as Ising models, and this tendency to order induces a nonzero order parameter in the nearby  $B$  films.

We conclude in Figs. 8 and 9 with sets of results for superlattices with layer thicknesses chosen to match those in the experimental studies. For  $N_A=19$  and  $N_B=6$ , we

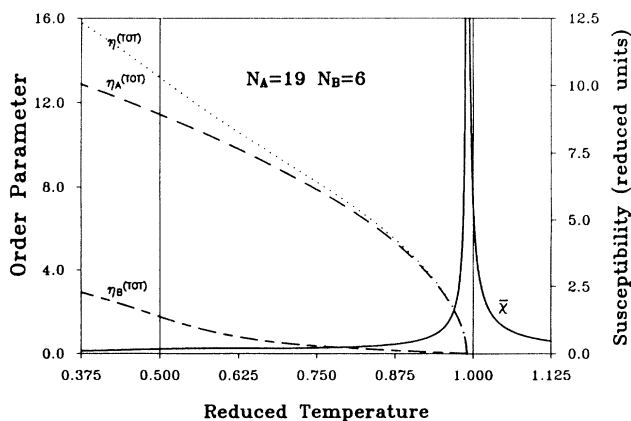


FIG. 8. Same as Fig. 2, except now  $N_A=19$ ,  $N_B=6$ , and  $T_A=0.9901$ .

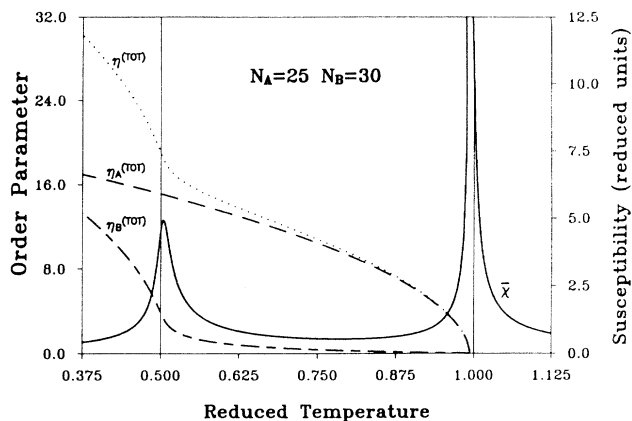


FIG. 9. Same as Fig. 2, except now  $N_A=25$ ,  $N_B=30$ , and  $T_A=0.9939$ ,  $T_B=0.5038$ .

see no evidence of structure in either  $\bar{\chi}$  or the order parameter near  $T_B^{(\infty)}$ , in agreement with experiment, while for  $N_A=25$  and  $N_B=30$ , we see a clear signature near  $T_B^{(\infty)}$ . Thus the experimental trends are reproduced nicely by these calculations.

A final question concerns the behavior of the order parameter in the  $B$  film, when there is strong structure in  $\bar{\chi}$  near  $T_B^{(\infty)}$ . We have given above the temperature variations of the order parameter integrated over the  $A$  and  $B$  film for the various examples considered. We show in Fig. 10 the spatial variation of the order parameter for  $N_A=10$  and  $N_B=40$ , for various temperatures in the near vicinity of the reduced temperature 0.5020, where  $\bar{\chi}$  has its maximum. Quite clearly, as the temperature is lowered through the maximum, the order parameter in the  $B$  film rises significantly. There is, however, a smooth variation near the maximum in  $\bar{\chi}$ . It would be difficult to

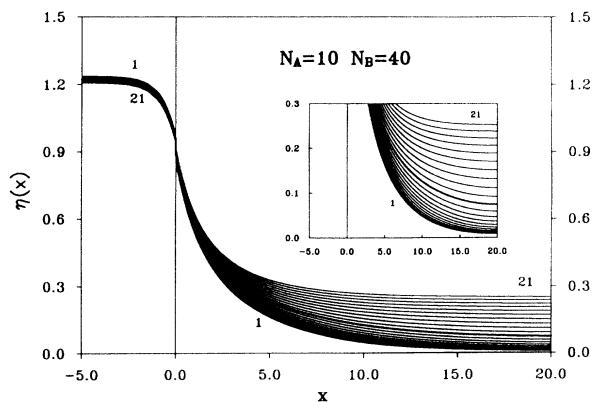


FIG. 10. For various temperatures on either side of the maximum in  $\bar{\chi}$  in Fig. 6, we show the spatial variation of the order parameter. There are 21 curves in the figure. Each curve corresponds to a temperature evenly spaced from 0.5145 to 0.4895, with curve 11 corresponding to the temperature 0.5020, at which  $\bar{\chi}$  have a maximum. The inset shows an enlarged portion of the curves.

deduce the temperature at which the peak occurs in  $\bar{\chi}$  from the information in this figure.

It would be of great interest to see further experimental studies of the response characteristics of superlattices near the ordering temperatures of their constituent films. Our calculations apply, for example, to a mean-field description of superlattices made from Fe and Ni. Studies of the temperature variation of the magnetization and of the susceptibility in the vicinity of the Ni Curie temperature, and that of Fe, would be of great interest. For this particular system, an important issue will be the integrity of the interfaces at these elevated temperatures.

In Sec. I, it was noted that Carriço and Camley<sup>2</sup> have

explored a microscopic model of  $\text{CoF}_2/\text{FeF}_2$  superlattices within mean-field theory. These authors compute the specific heat (and order parameters) in zero applied field, and inquire into the circumstances where a single structure is present and when two are found. Although our calculation is carried out within a very different theoretical framework than theirs, broadly speaking, the results of the two studies are quite similar.

#### ACKNOWLEDGMENT

This research was supported by the U. S. Army Research Office, through Contract No. CS001028.

---

<sup>1</sup>C. A. Ramos, D. Lederman, A. R. King, and V. Jaccarino, *Phys. Rev. Lett.* **65**, 2913 (1990).

<sup>2</sup>A. S. Carriço and R. E. Camley (unpublished).

<sup>3</sup>B. Heinrich, S. T. Purcell, J. R. Dutcher, K. B. Urquhart, J. F. Cochran, and A. S. Arrott, *Phys. Rev. B* **38**, 12 879 (1988).

<sup>4</sup>In the case of superconductors, there is no external field available that couples to the order parameter.

<sup>5</sup>P. G. de Gennes, *Superconductivity of Metals and Alloys* (Benjamin, New York, 1966), p. 235.